Expansion of Perception Area in Cellular Automata Using Recursive Algorithm

Yoshihiko Kayama

Department of Media and Information, BAIKA Women's University
2-19-5 Shukuno-sho, Ibaraki 567-8578, Osaka, Japan
y_kayama@ieee.org

Abstract

This study aims to present a new idea to expand the perception area of each cell in cellular automaton (CA) using a recursive algorithm known as "Recursive Estimation of Neighbors." An intelligent cellular process defined by the algorithm makes it possible to introduce an extra radius of the perception area, in addition to the radius of the CA neighborhood. A basic CA rule is extrapolated into rules with larger radii, which form a sequence indexed by the extra radius containing the basic CA as the first term of the sequence. The patterns formed in some typical sequences of extrapolated ECA and Life-like CA rules are presented. Contrasting pattern activities contained in homogeneous and heterogeneous CAs are discussed by applying mean field analysis. Some symmetrical arrangements of composites of cells with different radii are used in order to discuss the heterogeneous CA. The new perspective presented here offers several possible applications for CA.

Introduction

Cellular automaton (CA) is characterized by a large number of cells and a synchronous update of all cell states according to a local rule. As a result, CA has been used to describe the complexity emerging from interactions among simple individuals following simple rules. The original concept of CA was introduced by von Neumann and Ulam for modeling biological self-reproduction (Neuman, 1966). In the 1970s, Conway developed a two-dimensional CA rule, which he called "the Game of Life," that exhibited complex behaviors evoking biological activities (Gardner, 1970 and Berlekamp, Conway, and Guy, 1982). In the 1980s, Wolfram studied one-dimensional CAs (Wolfram, 1983, 1984, 1986, 2002), and proposed that CA could be grouped into four classes of complexity: homogeneous (class I), periodic (class II), chaotic (class III), and complex (class IV). This study mainly discusses a possibility to extend intelligence of each cell and presents a new perspective of CA for discussing relationship between information processing and pattern formation.

If intelligence can be described as the ability to perceive information and use it to form adaptive behaviors within an environment, each cell of CA seems not intelligent because it does not incorporate a process for organizing the information to determine its own future state. It is rather important that even such a simple model can simulate complex patterns reminding biological activities. In contrast, in a flocking boids simulation, which is a typical model of multi-agent system developed by Reynolds (Reynolds, 1987, and Banks, Vincent, and Anyakoha, 2007), each boid obtains the motion information of other boids within its perception area and using a simple algorithm, alters its own motion according to an analysis of this information. Boids easily organize themselves into a large, orderly group and move as a single organism without a central commander, i.e., their information processing leads to a collective control of the group motion. There seem to be a crucial difference between the two models, CA and the boids.

Actually, a framework inspired by that of boids, named the *Recursive Estimation of Neighbors* (REN), was introduced into CA to construct a model for studying the relationship between information processing and pattern formation in collective systems at *the 21st AROB international conference* (Kayama, 2016). In the present study, this idea is clarified and the formations of some interesting patterns in the studied CAs are investigated. It can be seen that the new model does not surpass the framework of CA but its reconstruction or reinterpretation. A basic CA rule with a unit rule radius is extrapolated into rules with larger radii through the REN algorithm. The extrapolated rules form a sequence indexed by an extra radius that represents the size of the perception area of a cell. The sequence contains the basic CA as its first term. When we call a CA model comprising cells with different values of the extra radius as *heterogeneous*, some models show interesting pattern formations. Contrasting examples in two-dimensional CA are discussed through the mean field analysis.

The next section shows how the intelligent process of each cell can be implemented using the REN algorithm, through the introduction of the extra radius in addition to the radius of the basic CA neighborhood. In Section 3, some typical sequences of the extrapolated CA rules in one-dimensional elementary CA (ECA) and two-dimensional eight-neighbor

outer-totalistic CA including Conway's Game of Life (Life-like CA) are presented. Sequences of ECA #22 and #110 modify their complexity between periodic and chaotic patterns depending on the even-odd parity of their extra index. In the extrapolated Game of Life sequence, there is a positive correlation between the extra radius and the average convergence speed to a rest state; however, in another sample sequence, there is a negative correlation. Such contrasting activities are interpreted by applying the mean field analysis in Section 4. Some interesting patterns are formed in heterogeneous models; their lattices are composed of cells that follow different extrapolated rules over a given sequence. Some geometrical arrangements of such different types of cells form composite models, which provide new application possibilities for CA.

Recursive Estimation of Neighbors

Practice is an activity to improve skills. When acquiring a skill, we initially try to recognize it as a set or some sequence of small actions. After repeating practice, such a process becomes unconscious, and the skill can be used just as a reflex action, in which no intelligent activities seem to be involved. An experienced person can deal with a lot of information almost automatically, whereas a beginner is likely to be at a standstill in front of it. If a CA rule is considered similar to such psychological insight, it might be possible to represent the rule by a set or some sequence of processes.

In case of boids, each boid acquires information regarding the positions and velocities of boids within its perception area and determines its own movement in order to follow the representative values of the neighbors. The radius of the perception area can be treated as a parameter expressing the differences between individual elements. In order to incorporate a similar scenario in CA, the perception area of a cell should be separated from the neighborhood determined by the CA rule, so that the size of the area can be treated as an attribute of each cell. Under the CA framework, however, the neighborhood of each cell is defined by the CA rule, and there is no possibility of expanding the sensory area of a cell. For example, each cell of ECA acquires the states of the three cells within its radius-one neighborhood to determine its state in the next timestep. The above psychological discussion suggests that such separation can be possible if the update process of each cell has an intermediate process of estimation of next states of neighboring cells as follows:

Acquire information of neighbors $\Rightarrow$ estimate their next states $\Rightarrow$ determine its own next state

Estimation and determination of states are assumed to be processed by only a basic CA rule because if other rules or mechanisms were introduced, the present framework would become complicated and difficult to find a reasonable selection method. Moreover, here we assume "self-similarity," which means that all cells use the same update algorithm. Then, the basic CA rule is expected to be used recursively.

Following the above discussion, the target framework includes the perception area for each cell in addition to the basic CA neighborhood. The states of all cells within the area are perceived in each timestep. Here we assume that the basic CA neighborhood and the perception area are both isotropic and can be parametrized by their radii r and R:

r**:** radius of the basic CA neighborhood shared by all cells.

R**:** radius depending on the size of the perception area of each cell.

The intelligent process of each cell is implemented by the REN algorithm, in which the basic CA rule is recursively used to estimate the states of the neighboring cells. The perceptual information of the states of cells inside the perception area of a cell should be consumed in an intelligent manner in the update process of the cell. The recursive usage of the basic CA rule continues until the state of the target cell is subsequently determined. Note that in the estimation process the values of the extra radius R of neighboring cells are assumed by the target cell and the assumed values are not necessarily identical with their actual ones.

The REN algorithm is defined as follows:

(i) In the estimation process, it is assumed that the same algorithm of recursive estimation is used by all neighboring cells (self-similarity). Within the perception area, each neighboring cell is assumed to have a perception area that is as large as possible.

(ii) In cases where the assumed perception area of a cell is smaller than the neighborhood of the basic CA rule ($R < r$), the cell in the next timestep is assumed to remain equal to the current state (termination condition).

Demonstrating the implementation in ECA, which is the simplest one-dimensional binary CA with $r = 1$, will help clarifying the REN concept. Here we suppose that an ECA model is *homogeneous*, which means that all cells have the same value of R.

The state of the i-th cell at timestep t and the ECA rule function are denoted by $x_i^{(t)}$ and f, respectively. The standard time evolution of the state is expressed by

$$x_i^{(t+1)} = f(x_{i-1}^{(t)}, x_i^{(t)}, x_{i+1}^{(t)}). \tag{1}$$

The new framework requires that the states of all neighboring cells at $t + 1$ are estimated by the ECA rule. Then the above expression changes to

$$\varphi_{R_0,i}^{(t+1)} = f(\varphi_{R_0-1,i-1}^{(t+1)}, x_i^{(t)}, \varphi_{R_0-1,i+1}^{(t+1)}), \tag{2}$$

where $\varphi_{R_0,i}^{(t+1)}$ is an estimated state of the i-th cell at $t + 1$ with radius $R = R_0$, and $\varphi_{R_0-1,i\pm1}^{(t+1)}$ are estimated states of the adjacent neighbors at $t + 1$ with an *assumed* radius

$R_0 - 1$; the value of the neighbors' radius stems from the above definition (i) because $R_0 - 1$ is the maximum value of the perception area for the neighbors within the perception area of the i-th cell with radius R_0. Note that $\varphi^{(t+1)}_{R_0,i}$ is assigned to the actual state $x^{(t+1)}_i$, but $\varphi^{(t+1)}_{R_0-1,i\pm1}$ are not necessarily equal to their respective actual states $x^{(t+1)}_{i\pm1}$ because the neighbors' true radius is not $R_0 - 1$, but R_0. Subsequently, the definition (i) leads to the following recursive expressions of the estimated states of the neighbors:

$$\varphi^{(t+1)}_{R_0-j,i-j} = f(\varphi^{(t+1)}_{R_0-j-1,i-j-1}, x^{(t)}_{i-j}, \varphi^{(t+1)}_{R_0-j-1,i-j+1}), \quad (3)$$

$$\varphi^{(t+1)}_{R_0-j,i+j} = f(\varphi^{(t+1)}_{R_0-j-1,i+j-1}, x^{(t)}_{i+j}, \varphi^{(t+1)}_{R_0-j-1,i+j+1}), \quad (4)$$

where $j = 1, 2, \ldots, R_0 - 1$. Because $j = R_0$ implies that the estimated value of R equals 0 ($< r = 1$), the definition (ii) gives the following conditions:

$$\varphi^{(t+1)}_{0,i\pm R_0} = x^{(t)}_{i\pm R_0}, \quad \varphi^{(t+1)}_{0,i\pm R_0\mp2} = x^{(t)}_{i\pm R_0\mp2}, \quad (5)$$

which terminate the above recursiveness.

As the first step of a concrete demonstration, let us consider the case $R_0 = r = 1$. Equations 2 and 5 give $x^{(t+1)}_i = f(\varphi^{(t+1)}_{0,i-1}, x^{(t)}_i, \varphi^{(t+1)}_{0,i+1})$ and $\varphi^{(t+1)}_{0,i\pm1} = x^{(t)}_{i\pm1}$. Accordingly, the ECA model with $R_0 = 1$ is identical to the basic ECA (Eq. 1). This discussion is not restricted to ECA; all CA models with $R_0 = r$ are identical to their basic CA. We next discuss the case $R_0 = 2$. Equation 2 gives $x^{(t+1)}_i = f(\varphi^{(t+1)}_{1,i-1}, x^{(t)}_i, \varphi^{(t+1)}_{1,i+1})$, and the recursive expressions 3 and 4 give

$$\varphi^{(t+1)}_{1,i-1} = f(\varphi^{(t+1)}_{0,i-2}, x^{(t)}_{i-1}, \varphi^{(t+1)}_{0,i}), \quad (6)$$

$$\varphi^{(t+1)}_{1,i+1} = f(\varphi^{(t+1)}_{0,i}, x^{(t)}_{i+1}, \varphi^{(t+1)}_{0,i+2}), \quad (7)$$

Because $\varphi^{(t+1)}_{0,i} = x^{(t)}_i$ and $\varphi^{(t+1)}_{0,i\pm2} = x^{(t)}_{i\pm2}$ from the termination conditions (Eqs. 5), the CA model with $R_0 = 2$ is expressed by

$$x^{(t+1)}_i = f(f(x^{(t)}_{i-2}, x^{(t)}_{i-1}, x^{(t)}_i), x^{(t)}_i, f(x^{(t)}_i, x^{(t)}_{i+1}, x^{(t)}_{i+2})), \quad (8)$$

which corresponds to a five-neighbor CA rule, $x^{(t+1)}_i = g(x^{(t)}_{i-2}, x^{(t)}_{i-1}, x^{(t)}_i, x^{(t)}_{i+1}, x^{(t)}_{i+2})$. Equation 8 is an "intelligent" expression of the rule g. The cases for larger values of R can be derived similarly.

The above discussion indicates that the REN algorithm with increasing sizes of perception areas indexed by R extrapolates the basic CA rule to rules with larger radius $r = 2 \times R + 1$. The extrapolated rules from the basic CA form a *sequence* parametrized by R. Namely, a CA rule included in the sequence can be reconstructed from the basic CA through REN, where each cell has its own perception area and acts as an intelligent agent.

Sequence of Extrapolated CA rules

When a basic CA is assigned to a code $\mathcal{N}$, a sequence of extrapolated rules from the basic CA with index R is represented by $[\mathcal{N}]$. If each CA included in the sequence should be identified, its code is shown as the basic CA code followed by the letter "R" and its value n. The sequence is represented by $[\mathcal{N}]$=$\{\mathcal{N}\mathrm{R}1, \mathcal{N}\mathrm{R}2, \mathcal{N}\mathrm{R}3, \ldots\}$, where $\mathcal{N}$R1 is identical with the basic CA. Each cell that belongs to $\mathcal{N}\mathrm{R}n$ is called an "$\mathcal{N}\mathrm{R}n$ cell."

The implementation of REN discussed in the previous section can be applied to Life-like CA. A pattern that does not change from one generation to the next is known as a "still life" in the Game of Life and other CA. The following property of the sequence of extrapolated CAs is proved:

- A still life in $\mathcal{N}$R1 is also a still life in any CA included in the sequence $[\mathcal{N}]$, when it is sufficiently isolated.

"Sufficiently isolated" means that any perception area of cells that form the located still life contains no active cells other than the member of the still life. To prove this property, we adopt the notation of the previous section. The generalization to other cases, e.g., Life-like CA, is straightforward.

(1) A pattern *SL* in $\mathcal{N}$R1 is assumed to be a still life, which means that for any cell i in *SL*,

$$x^{(t+1)}_i = \varphi^{(t+1)}_{1,i} = f(x^{(t)}_{i-1}, x^{(t)}_i, x^{(t)}_{i+1}) = x^{(t)}_i.$$

(2) In $\mathcal{N}$R2, any state x_i follows

$$x^{(t+1)}_i = \varphi^{(t+1)}_{2,i} = f(\varphi^{(t+1)}_{1,i-1}, x^{(t)}_i, \varphi^{(t+1)}_{1,i+1}).$$

From (1) and the assumption "sufficiently isolated," $x^{(t+1)}_{i\pm1} = \varphi^{(t+1)}_{1,i\pm1} = x^{(t)}_{i\pm1}$ are also satisfied in *SL*. Then,

$$x^{(t+1)}_i = f(x^{(t)}_{i-1}, x^{(t)}_i, x^{(t)}_{i+1}) = x^{(t)}_i.$$

(3) If *SL* is assumed to be a still life in $\mathcal{N}\mathrm{R}n$, then

$$x^{(t+1)}_i = \varphi^{(t+1)}_{n,i} = x^{(t)}_i.$$

(4) In $\mathcal{N}\mathrm{R}(n+1)$, any state x_i follows

$$x^{(t+1)}_i = \varphi^{(t+1)}_{n+1,i} = f(\varphi^{(t+1)}_{n,i-1}, x^{(t)}_i, \varphi^{(t+1)}_{n,i+1}).$$

From (3) and the assumption "sufficiently isolated," $x^{(t+1)}_{i\pm1} = \varphi^{(t+1)}_{n,i\pm1} = x^{(t)}_{i\pm1}$ are also satisfied in *SL*. Then from (1),

$$x^{(t+1)}_i = f(x^{(t)}_{i-1}, x^{(t)}_i, x^{(t)}_{i+1}) = x^{(t)}_i.$$

Although pattern formations in sequences of extrapolated ECA and Life-like CA were already demonstrated in Kayama, 2016, some typical examples are presented in the following subsections.

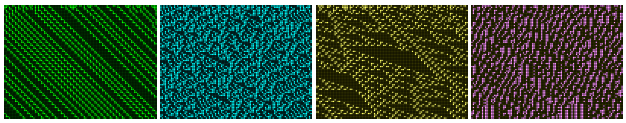

Figure 1: Patterns in [#134]: R1, R2, R3, R4 (left to right).

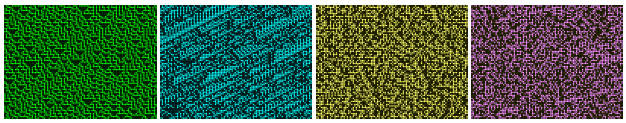

Figure 2: Patterns in [#30]: R1, R2, R3, R4 (left to right).

Extrapolated ECA

ECA is the simplest nontrivial CA with $r = 1$; its $2^3 = 8$ different neighborhood configurations result in $2^8 = 256$ possible rules. We follow the standard naming convention invented by Wolfram (Wolfram, 1983, 2002), which assigns each ECA rule a number from #0 to #255. The equivalency of the CA rules under mirror and complementary transformations reduces the number of independent rules to 88 (Li and Packard, 1990, and Kayama, 2011). In the simulations used in this subsection, we set the maximum value of R to 20. Among the sequences generated from independent ECA rules, eight are based on class I rules and all of the rules contained in these sequences also belong to class I. In contrast, various pattern formations can be found in sequences based on class II rules. The sequence [#134] shows changes between periodic and chaotic patterns depending on the index R (Fig. 1), where the colored dots are live cells and the black ones are dead. The patterns originate from pseudo-randomly generated initial configurations. The initial probability of live cells is set to 0.5. Pattern formations in sequences based on class III and IV rules are also attractive. Class III rules are sometimes exemplified by rule #30, and its sequence [#30] exhibits chaotic patterns (Fig. 2). Especially, the patterns with large R values (#30R3 and R4) are typical ones. For example, the pattern of #90R2 in Fig. 3a cannot be distinguished from them. But the pattern of rule #18 is sparser (Fig. 3b). Some sequences show periodic changes between periodic and chaotic patterns depending on the even-odd parity of R, e.g., [#22] (Fig. 4) and [#110] (Fig. 5). In these cases, no simple correlations are found between fluctuation control and the radius R, even when the amount of information each cell acquires increases monotonically with R.

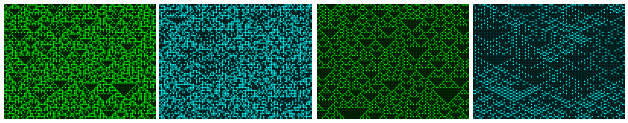

(a) Left: #90R1, right: #90R2 (b) Left: #18R1, right: #18R2

Figure 3: Patterns in (a) [#90] and (b) [#18].

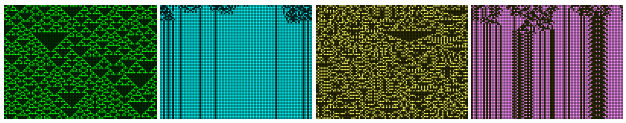

Figure 4: Patterns in [#22]: R1, R2, R3, R4 (left to right).

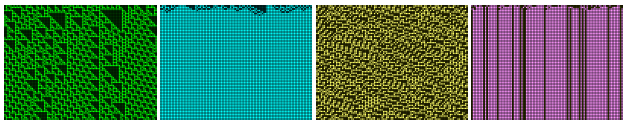

Figure 5: Patterns in [#110]: R1, R2, R3, R4 (left to right).

Extrapolated Life-like CA

In the descriptions below, all Life-like CA rules are specified in the Golly/RLE format (Adamatzky (Ed.), 2010, and Eppstein, 2010). The Game of Life is denoted by B3S23 in this notation, where "B" stands for "birth" and "S" stands for "survival." In the Game of Life, many complex patterns and activities can emerge (Callahan, 1995, and Flammenkamp, 1998). After a long transient process, a randomly generated initial configuration is transferred to a rest state that can include various patterns: still lifes (e.g., blocks, beehives, or ships) and oscillators (e.g., blinkers, toads, or beacons). Any isolated still life is also still life in any extrapolated rule, as proved above. Figure 6a shows the rest states of [B3S23]. In contrast, [B23S234] has a stable state only in B23S234R1 and random states in all others (Fig. 6b). Their randomness gradually increases with R. These contrasting examples are investigated in the mean field analysis in the next section.

Mixing Cells with Different R

Thus far, only homogeneous CAs were discussed, in which all the cells follow the same rule with the same value of R. If we note that the extra radius R is an index of the amount of

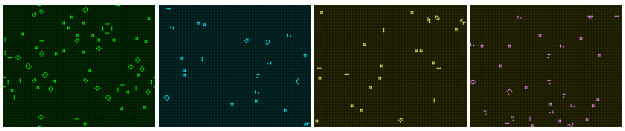

(a) [B3S23]: R1, R2, R3, R4 (left to right).

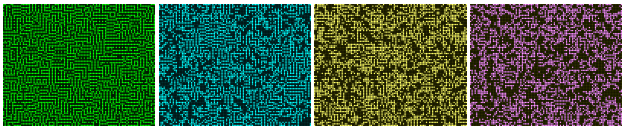

(b) [B23S234]: R1, R2, R3, R4 (left to right).

Figure 6: Patterns in homogeneous (a) [B3S23] and (b) [B23S234]

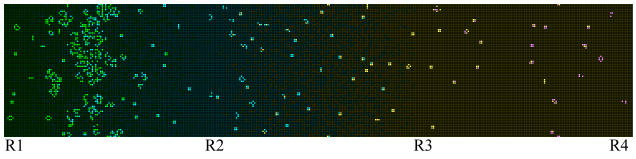

(a) B3S23R1⇒R2⇒R3⇒R4

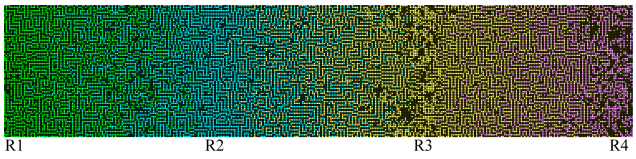

(b) B23S234R1⇒R2⇒R3⇒R4

Figure 7: Mixings of cells with different R in (a) [B3S23] and (b) [B23S234]

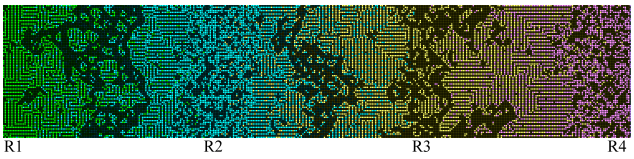

Figure 8: Mixing of cells with different R in [B4S1234]: R1⇒R2⇒R3⇒R4.

information each cell can acquire, R can be recognized as a characteristics of a cell and heterogeneous CA composed of cells with different values of R become meaningful. Figures 7a and 7b present the mixing of cells with different values of R in [B3S23] and [B23S234], respectively. The mixing ratio between two kinds of cells, Rn:R$(n+1)$, changes linearly from 1:0 to 0:1. Although homogeneous B3S23R1 and R2 have rest states as shown in Fig. 6a, Fig. 7a shows an emergence of unstable states in their intermediate mixing area. In contrast, Fig. 7b shows that all mixing areas of [B23S234] become stable. The difference between them is also discussed in the next section.

A heterogeneous CA in [B4S1234] is also interesting. Figure 8 shows a complex pattern change; areas of islands and random states are sandwiched between walls. Their mixing ratio is the same as in the case of Fig. 7, but the initial probability of live cells is set to 0.2.

Mean Field Analysis

Mean field analysis assumes that the iterative application of a rule does not introduce correlations between states of cells in different positions when applied to CA (Wolfram, 1983, Schulman and Seiden, 1978). This assumption is generally not valid, but allows the derivation of a simple formula for investigating the qualitative behavior of CA dynamics and an estimation of the limit density of the possible states of a cell. Mean field analysis is applied to the contrasting examples of [B3S23] and [B23S234] presented in the previous section.

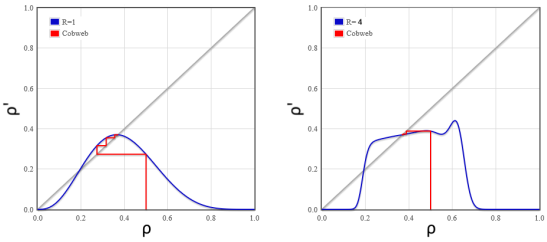

(a) B3S23R1 (b) B3S23R4

Figure 9: CobWeb plots of [B3S23]

Homogeneous CA

A Life-like CA rule is determined by the numbers of "births" and "survivals." Here they are symbolized by *bth* and *svl*, respectively. The time evolution relationship (Eq. 2) is rewritten in the mean field analysis as follows:

$$\rho'_{R_0} = (1-\rho_{R_0})B(\rho'_{eR_0-1}, bth) + \rho_{R_0}S(\rho'_{eR_0-1}, svl), \tag{9}$$

where ρ and ρ' are the densities of the live cells at the present and at the next timestep, respectively. ρ'_{eR_0-1} is the estimated density of live cells relating to $\varphi^{(t+1)}_{R_0-1}$. The functions B and S refer to the contributions from the eight neighboring cells according to the rule. The recursive expressions, Eqs. 3 and 4, lead to

$$\rho'_{eR_0-j} = (1-\rho_{R_0})B(\rho'_{eR_0-j-1}, bth)+\rho_{R_0}S(\rho'_{eR_0-j-1}, svl). \tag{10}$$

where $j = 1, 2, \ldots, R_0 - 1$. Because the termination conditions (Eqs. 5) give $\rho'_{e0} = \rho_{R_0}$, the above Eq. 10 leads to

$$\rho'_{e1} = (1-\rho_{R_0})B(\rho_{R_0}, bth) + \rho_{R_0}S(\rho_{R_0}, svl). \tag{11}$$

A recursive use of Eq. 10 and Eq. 11 in Eq. 9 derive a relational expression between ρ'_{R_0} and ρ_{R_0}. In B3S23, the Game of Life , the functions B and S are expressed by

$$\begin{aligned} B(\rho, 3) &= \binom{8}{3}\rho^3(1-\rho)^5, \\ S(\rho, 23) &= B(\rho, 3) + \binom{8}{2}\rho^2(1-\rho)^6. \end{aligned}$$

Mean field diagrams and cobweb plots of B3S23R1 and R4 are presented in Fig. 9, where the number of timesteps for reaching the limit density from the initial density 0.5 decreases with the value of R. This result means that there can be a positive correlation between the average convergence

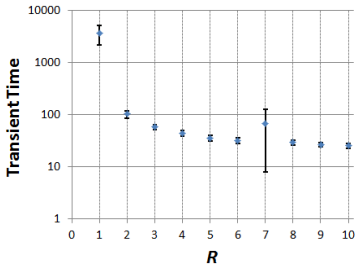

Figure 10: Semi-log plots of transient times in [B3S23]. Each error bar indicates the standard deviation.

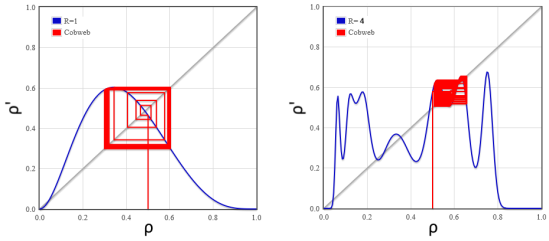

(a) B23S234R1 (b) B23S234R4

Figure 11: CobWeb plots of [B23S234]

speed and the value of R, namely the size of the perception area. Actually, Fig. 10 shows that the average transient time from fifty pseudo-randomly generated initial configurations on a 200×160 lattice to rest states decreases[1]. In contrast, the mean field diagrams and the cobweb plots of [B23S234] become complex with the value of R. Accordingly, the cell states become unstable (Fig. 7b). In other words, the REN algorithm in [B3S23] consumes information of cell states efficiently to control the fluctuations of the states, but that in [B23S234] disturbs the cell states.

Heterogeneous CA

As pointed out in Section 3.3, the pattern formations in the heterogeneous CAs in [B3S23] and [B23S234] are contrasting. In order to discuss them through mean field analysis, some geometrical symmetry is required to the arrangement of cells with different R.

The definition (i) of REN results in a specific composite configuration of cells. If an R2 cell is surrounded by eight R1 cells (Fig. 12a), the estimation of the states of the neighboring cells from the center cell is always correct, which means that the nine cells can be considered as one composite with 2^9 states. In the symmetrical arrangement of Fig. 12b, all R1 cells have seven R1 and one R2 neighbors, and all R2 cells have eight R1 neighbors. Then these two kinds of cells can be represented by two densities of cells ρ_1 and

[1]The long transient time at $R = 6$ is the only exception owing to a glider (Kayama, 2016).

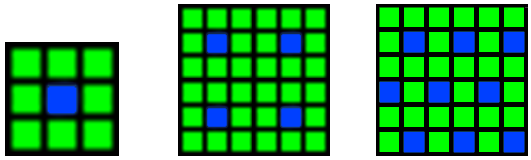

(a) (b) R1:R2=8:1 (c) R1:R2=4:1

Figure 12: (a) Composite configuration comprising one center cell ($R = 2$; blue) and eight neighboring cells ($R = 1$; green), and its symmetrical arrangements; the ratios of the numbers of R1 and R2 cells are (b) 8:1 and (c) 4:1.

ρ_2 in the mean field analysis, respectively. ρ_1 satisfies the following expression:

$$\rho'_1 = (1-\rho_1)B(\rho_1,\rho_2,bth) + \rho_1 S(\rho_1,\rho_2,svl), \quad (12)$$

where the termination conditions are taken into account. B and S are expressed in [B3S23] as follows:

$$\begin{aligned} B(\rho_1,\rho_2,3) &= \binom{7}{2}\rho_1^2(1-\rho_1)^5\rho_2 \\ &\quad + \binom{7}{3}\rho_1^3(1-\rho_1)^4(1-\rho_2), \\ S(\rho_1,\rho_2,23) &= B(\rho_1,\rho_2,3) + \binom{7}{1}\rho_1(1-\rho_1)^6\rho_2 \\ &\quad + \binom{7}{2}\rho_1^2(1-\rho_1)^5(1-\rho_2). \end{aligned}$$

The expression of ρ_2 comes from Eq. 9 as follows:

$$\rho'_2 = (1-\rho_2)B(\rho_{e1},bth) + \rho_2 S(\rho_{e1},svl), \quad (13)$$

where the density of the estimated state ρ_{e1} is identical with ρ'_1, because the estimation of the states of the neighboring R1 cells from the R2 cell is always correct. The numerical results of iterations of the above expressions 12 and 13 in [B3S23] lead to Fig. 13, which shows that the symmetrical arrangement of Fig. 12b has no essential differences with the homogeneous B3S23R2. In contrast, the plots of the numerical results of the above expressions of the arrangement of B23S234R1 and R2 cells and homogeneous B23S234R2 are totally different. Correlation between R1 and R2 cells suppresses their fluctuation mutually and their densities approach a limit value. These results correspond to pattern formations in the symmetrical arrangements of B3S23R1 and R2 cells and B23S234R1 and R2 cells. The former reaches a rest state and the latter a stable one.

In order to understand the emergence of unstable states in the mixing area between B3S23R1 and R2 in Fig. 7a, we adopt another symmetrical arrangement of Fig. 12c. Actually, the pattern formation in this arrangement is unstable

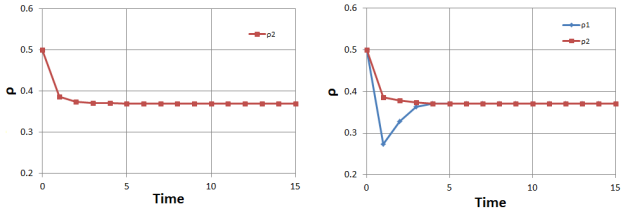

(a) (b)

Figure 13: Plots of iterations in (a) homogeneous B3S23R2 and (b) composite of R1:R2=8:1

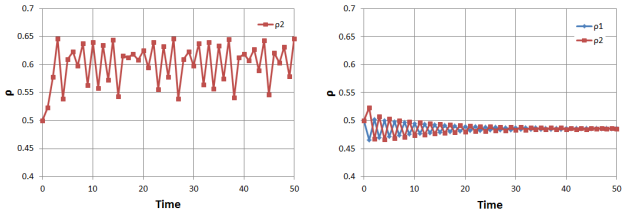

(a) (b)

Figure 14: Plots of iterations in (a) homogeneous B23S234R2 and (b) arrangement of B23S234R1:R2=8:1

(Fig. 15a). The arrangement requires two kinds of R1 cells and one R2 cell. If the two kinds of R1 cells are represented by Ra and Rb, they are distinguished by their neighbors; Ra cell has six Rb and two R2 neighbors, and Rb cell has three Ra, two Rb and three R2 neighbors. R2 cell has two Ra and six Rb neighbors. If the densities of the three types of cells are denoted by ρ_a, ρ_b, and ρ_2, they satisfy the following expressions:

$$\rho'_a = (1-\rho_a)B_a(\rho_b,\rho_2,3) + \rho_a S_a(\rho_b,\rho_2,23), \quad (14)$$

$$\rho'_b = (1-\rho_b)B_b(\rho_a,\rho_b,\rho_2,3) + \rho_b S_b(\rho_a,\rho_b,\rho_2,23), \quad (15)$$

$$\rho'_2 = (1-\rho_2)B_2(\rho_a,\rho_b,3) + \rho_2 S_2(\rho_a,\rho_b,23), \quad (16)$$

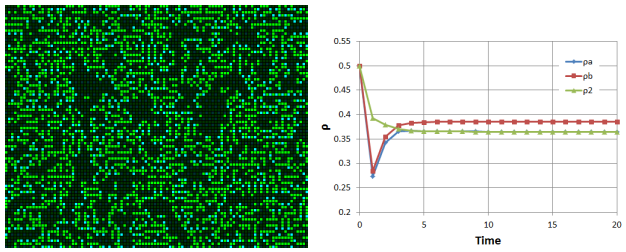

(a) (b)

Figure 15: (a) Unstable pattern in the symmetrical arrangement (Fig. 12c) of B3S23R1:R2=4:1 composites and (b) its plot of iterations.

where the above functions, Bs and Ss, are presented in Table 1. The plot of the numerical results is shown in Fig. 15b. The existence of a gap between ρ_a and ρ_b represents the existence of the unstable area.

From the above discussion, mean field analysis can be effective to investigate the qualitative behavior of heterogeneous CA, if some symmetrical arrangements of the composites are adopted.

Conclusions

The REN algorithm allows for defining the intelligent process of each cell by introducing an extra index R that represents the radius of the perception area of a cell in addition to the radius of the CA neighborhood. A basic CA rule with a unit rule radius is extrapolated into rules with larger radii $r = 2 \times R + 1$, which form a sequence indexed by R containing the basic CA as the first term of the sequence. Pattern formations in some typical sequences of the extrapolated ECA and Life-like CA rules are presented. It is proven that a still life in the basic CA is also a still life in any extrapolated rule over the same sequence when the still life is sufficiently isolated. The sequence of the Game of Life ([B3S23]) and [B23S234] exhibit the contrasting activities of cell states, which are discussed through mean field analysis. Those mean field diagrams show opposite effects of their extrapolations in accordance with R. Namely, the REN algorithm in [B3S23] consumes information about the cell states efficiently in order to control the fluctuations of the states, but that in [B23S234] disturbs the cell states. The pattern activities of the heterogeneous models of mixing R1 and R2 cells in [B3S23] and [B23S234] are also contrasting. Some symmetrical arrangements of the composites containing R2 cells surrounded by eight R1 cells are examined to discuss the models in the mean field analysis. The unstable area between B3S23R1 and R2 may be emerged from the gap between the limit densities of two kinds of R1 cells. The stable area between B23S234R1 and R2 comes from mutually suppressing their fluctuations. Correspondingly, mean field analysis of their densities shows that they approach to the same limit value. Furthermore, mean field analysis is effective in investigating qualitative behavior of heterogeneous CA, not just homogeneous CA.

The new perspective of CA presented here has several different potential applications. Heterogeneous CAs with combinations of cells with different values of R show unexpected pattern activities. Such phenomena appear to act like mixing two different materials; the end material has a changed state by the chemical process. The symmetrical arrangements of composites could be related to crystal substances in solid-state physics. If interactions between cells and an evolutionary algorithm are introduced in the heterogeneous CA, a new theoretical field, like "CA Chemistry," could be established just as the boids theory was developed to "Swarm Chemistry" (Sayama, 2007, 2009, 2010).

$$
\begin{aligned}
&B_a(\rho_b,\rho_2,3) = \tbinom{6}{1}\rho_b(1-\rho_b)^5\rho_2^2 \\
&\quad +\tbinom{6}{2}\rho_b^2(1-\rho_b)^4\tbinom{2}{1}\rho_2(1-\rho_2) + \tbinom{6}{3}\rho_b^3(1-\rho_b)^3(1-\rho_2)^2 \\
&S_a(\rho_b,\rho_2,23) = B_a + (1-\rho_b)^6\rho_2^2 \\
&\quad +\tbinom{6}{1}\rho_b(1-\rho_b)^5\tbinom{2}{1}\rho_2(1-\rho_2) + \tbinom{6}{2}\rho_b^2(1-\rho_b)^4(1-\rho_2)^2 \\
&B_b(\rho_a,\rho_b,\rho_2,3) = (1-\rho_a)^3(1-\rho_b)^2\rho_2^3 \\
&\quad +(1-\rho_a)^3\tbinom{2}{1}\rho_b(1-\rho_b)\tbinom{3}{2}\rho_2^2(1-\rho_2) \\
&\quad +\tbinom{3}{1}\rho_a(1-\rho_a)^2(1-\rho_b)^2\tbinom{3}{2}\rho_2^2(1-\rho_2) \\
&\quad +\left\{(1-\rho_a)^3\rho_b^2 + \tbinom{3}{2}\rho_a^2(1-\rho_a)(1-\rho_b)^2\right\}\tbinom{3}{1}\rho_2(1-\rho_2)^2 \\
&\quad +\tbinom{3}{1}\rho_a(1-\rho_a)^2\tbinom{2}{1}\rho_b(1-\rho_b)\tbinom{3}{1}\rho_2(1-\rho_2)^2 \\
&\quad +\left\{\tbinom{3}{1}\rho_a(1-\rho_a)^2\rho_b^2 + \rho_b^3(1-\rho_b)^2\right\}(1-\rho_2)^3 \\
&\quad +\tbinom{3}{2}\rho_a^2(1-\rho_a)\tbinom{2}{1}\rho_b(1-\rho_b)(1-\rho_2)^3 \\
&S_b(\rho_a,\rho_b,\rho_2,23) = B_b + (1-\rho_a)^3(1-\rho_b)^2\tbinom{3}{2}\rho_2^2(1-\rho_2) \\
&\quad +(1-\rho_a)^3\tbinom{2}{1}\rho_b(1-\rho_b)\tbinom{3}{1}\rho_2(1-\rho_2)^2 \\
&\quad +\tbinom{3}{1}\rho_a(1-\rho_a)^2(1-\rho_b)^2\tbinom{3}{1}\rho_2(1-\rho_2)^2 \\
&\quad +\left\{(1-\rho_a)^3\rho_b^2 + \tbinom{3}{2}\rho_a^2(1-\rho_a)(1-\rho_b)^2\right\}(1-\rho_2)^3 \\
&\quad +\tbinom{3}{1}\rho_a(1-\rho_a)^2\tbinom{2}{1}\rho_b(1-\rho_b)(1-\rho_2)^3 \\
&B_2(\rho_a,\rho_b,3) = (1-\rho_a)^2\tbinom{6}{3}\rho_b^3(1-\rho_b)^3 \\
&\quad +\tbinom{2}{1}\rho_a(1-\rho_a)\tbinom{6}{2}\rho_b^2(1-\rho_b)^4 + \rho_a^2\tbinom{6}{1}\rho_b(1-\rho_b)^5 \\
&S_2(\rho_a,\rho_b,23) = B_2 + (1-\rho_a)^2\tbinom{6}{2}\rho_b^2(1-\rho_b)^4 \\
&\quad +\tbinom{2}{1}\rho_a(1-\rho_a)\tbinom{6}{1}\rho_b(1-\rho_b)^5 + \rho_a^2(1-\rho_b)^6
\end{aligned}
$$

Table 1: Contribution functions Bs and Ss in mean field analysis for the symmetrical arrangement of B3S23R1 and R2 cells (Eqs. 14-16).

Acknowledgments

The author wishes to thank Y. Imamura and the all anonymous reviewers for valuable comments and suggestions.

References

Adamatzky, A., editor (2010). *Game of life cellular automata*. London:: Springer.

Banks, A., Vincent, J., and Anyakoha, C. (2007). A review of particle swarm optimization. part i: background and development. *Natural Computing*, 6.4:467–484.

Berlekamp, E. R., Conway, J. H., and Guy, R. K. (1982). *Winning Ways for Your Mathematical Plays*. Academic, New York.

Callahan, P. (1995). Patterns, programs, and links for conway's game of life. "`http://www.radicaleye.com/lifepage/`". Retrieved at February 1, 2011.

Eppstein, D. (2010). Growth and decay in life-like cellular automata. In Adamatzky, A., editor, *Game of Life Cellular Automata*, pages 71–98. Springer.

Flammenkamp, A. (1998). Achim's game of life. "`http://wwwhomes.uni-bielefeld.de/achim/gol.html`". Retrieved at December 12, 2011.

Gardner, M. (1970). Mathematical games. *Scientific American*, 223:102–123.

Kayama, Y. (2011). Network representation of cellular automata. In *2011 IEEE Symposium on Artificial Life (IEEE ALIFE 2011) at SSCI 2011*, pages 194–202.

Kayama, Y. (2016). Extension of cellular automata by introducing an algorithm of recursive estimation of neighbors. In *Proceedings of the 21-st International Symposium on Artificial Life and Robotics*, pages 73–77.

Li, W. and Packard, N. (1990). The structure of the elementary cellular automata rule space. *Complex Systems*, 4:281–297.

Reynolds, C. W. (1987). Flocks, herds and schools: A distributed behavioral model. *ACM Siggraph Computer Graphics*, 21.4:25–34.

Sayama, H. (2007). Decentralized control and interactive design methods for large-scale heterogeneous self-organizing swarms. *Advances in Artificial Life*, 15(1):105–114.

Sayama, H. (2009). Swarm chemistry. *Artificial Life*, 15.1:105–114.

Sayama, H. (2010). Robust morphogenesis of robotic swarms. *Computational Intelligence Magazine, IEEE*, 5(3):43–49.

Schulman, L. S. and Seiden, P. E. (1978). Statistical mechanics of a dynamical system based on conway's game of life. *Journal of Statistical Physics*, 19(3):293–314.

von Neumann, J. (1966). The theory of self-reproducing automata. In Burks, A. W., editor, *Essays on Cellular Automata*. University of Illinois Press.

Wolfram, S. (1983). Statistical mechanics of cellular automata. *Rev. Mod. Phys.*, 55:601–644.

Wolfram, S. (1984). Universality and complexity in cellular automata. *Physica D*, 10:1–35.

Wolfram, S. (1986). *Theory and Applications of Cellular Automata*. World Scientific, Singapore.

Wolfram, S. (2002). *A New Kind of Science*. Wolfram Media, Inc.